Electronic Supplementary Material (ESI) for Journal of Materials Chemistry A.

Unraveling the Role of Bonding Chemistry in Connecting Electronic and Thermal Transport by Machine Learning

Rinkle Juneja and Abhishek K. Singh*

Materials Research Centre, Indian Institute of Science, Bangalore 560012, India

E-mail: abhishek@iisc.ac.in

*To whom correspondence should be addressed

Electronic transport properties for the screened compounds

For all the screened compounds, electronic transport properties are calculated. The room temperature Seebeck coefficient S and scaled electrical conductivity $\frac{\sigma}{\tau}$ over the carrier concentration range 10^{19} to 10^{22} cm^{-3} are shown in Figures S1-S3 and Figures S4-S6.

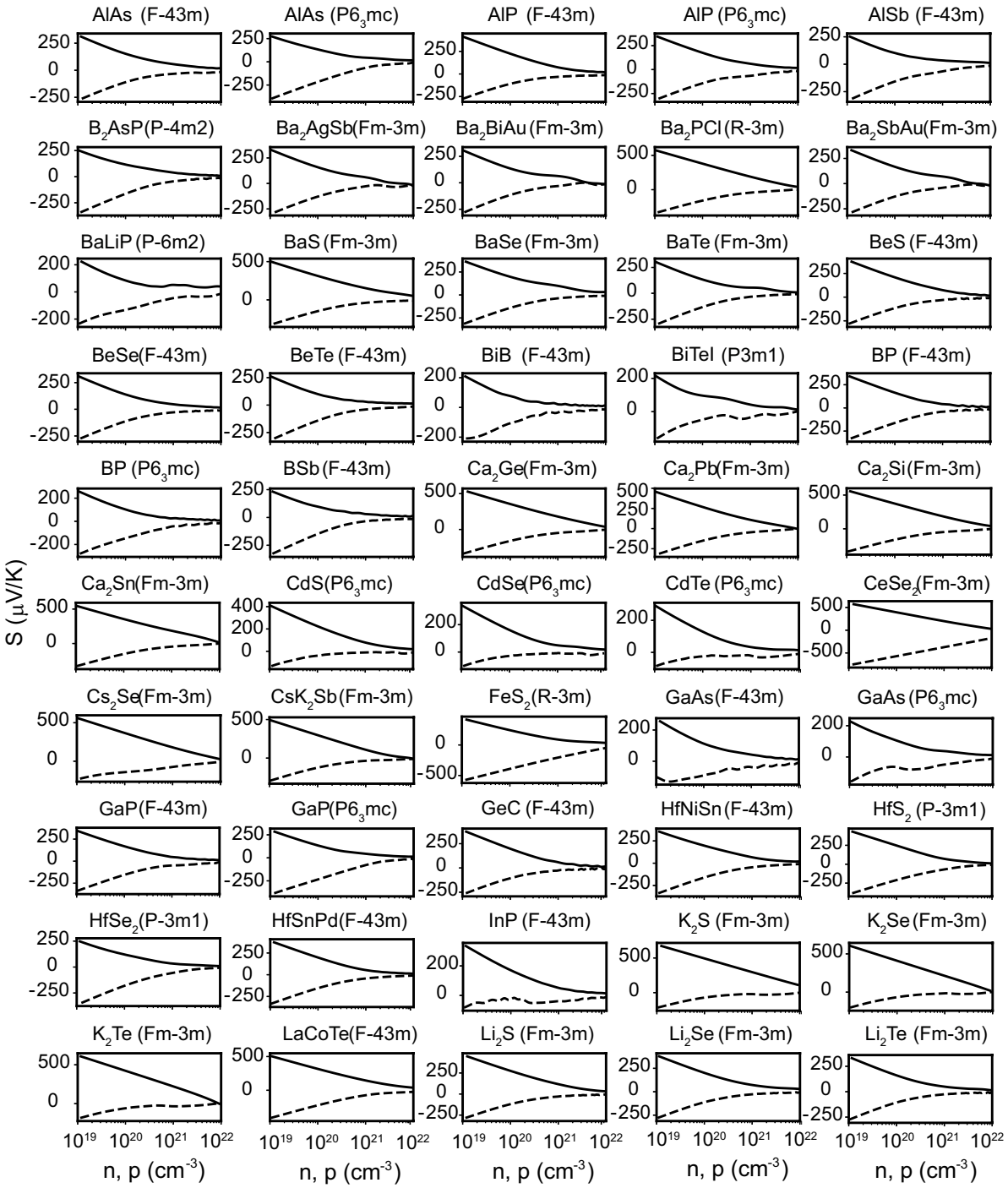

Figure 1: Calculated Seebeck coefficient S as a function of carrier concentration at room temperature.

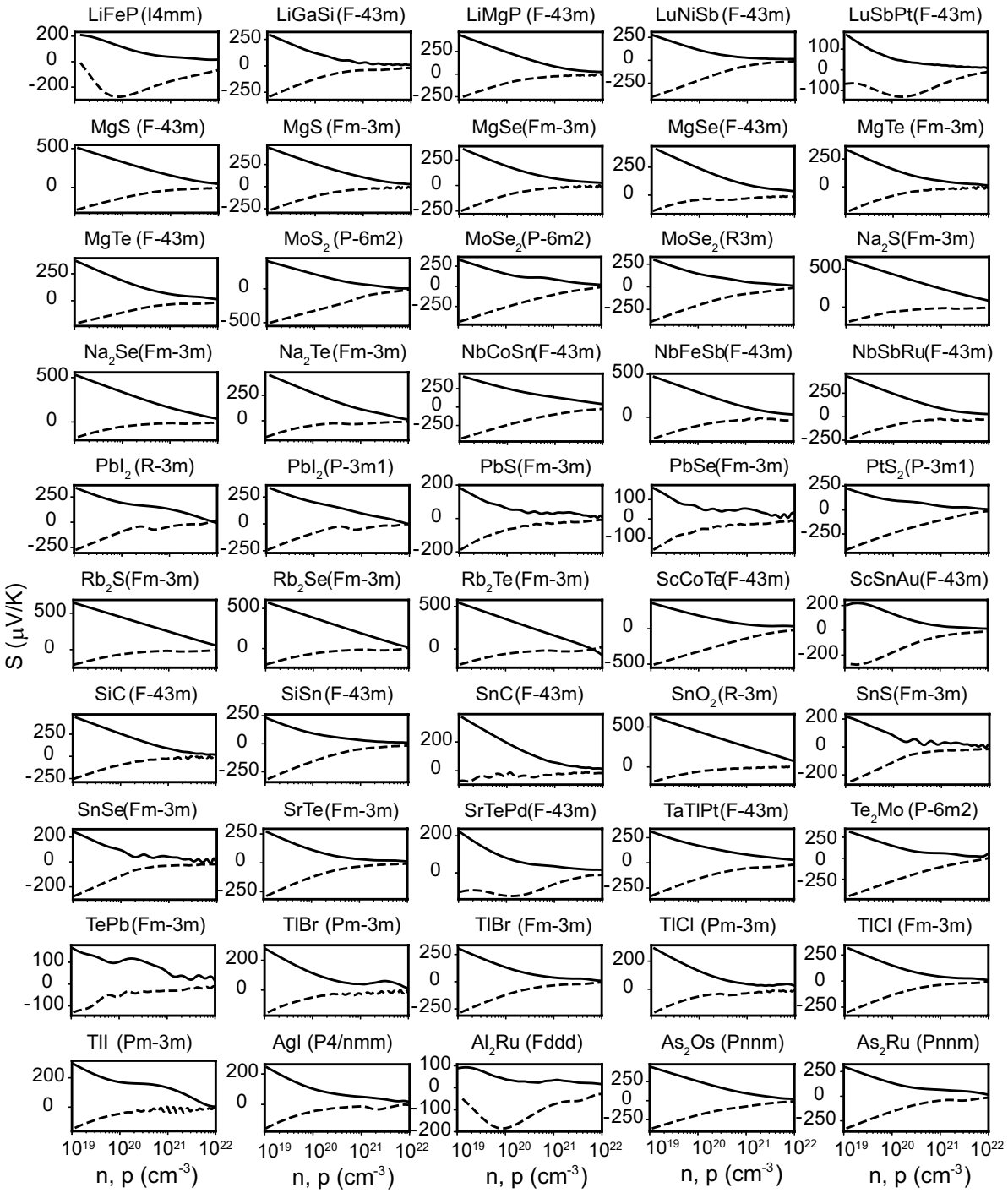

Figure 2: Calculated Seebeck coefficient S as a function of carrier concentration at room temperature.

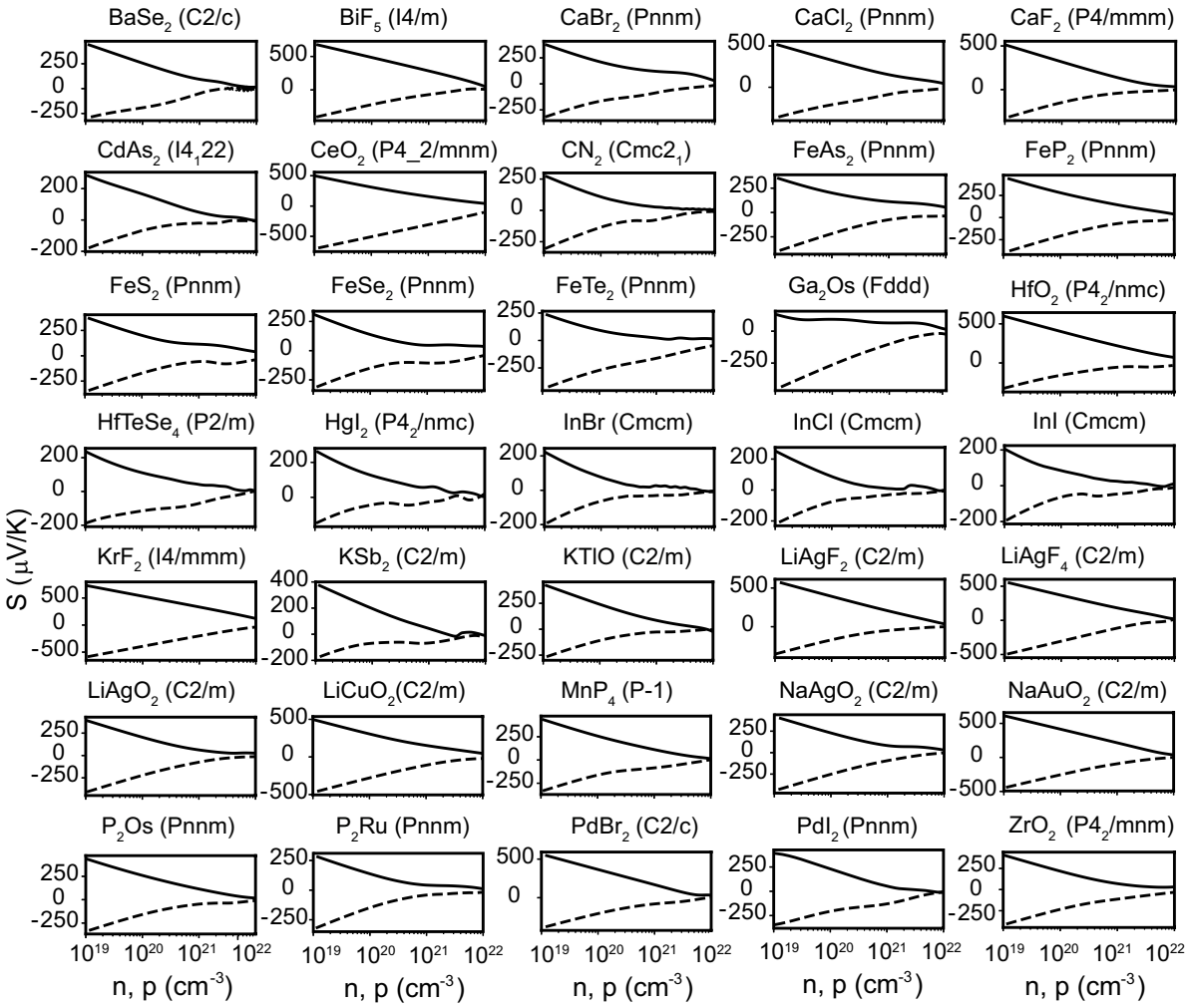

Figure 3: Calculated Seebeck coefficient S as a function of carrier concentration at room temperature.

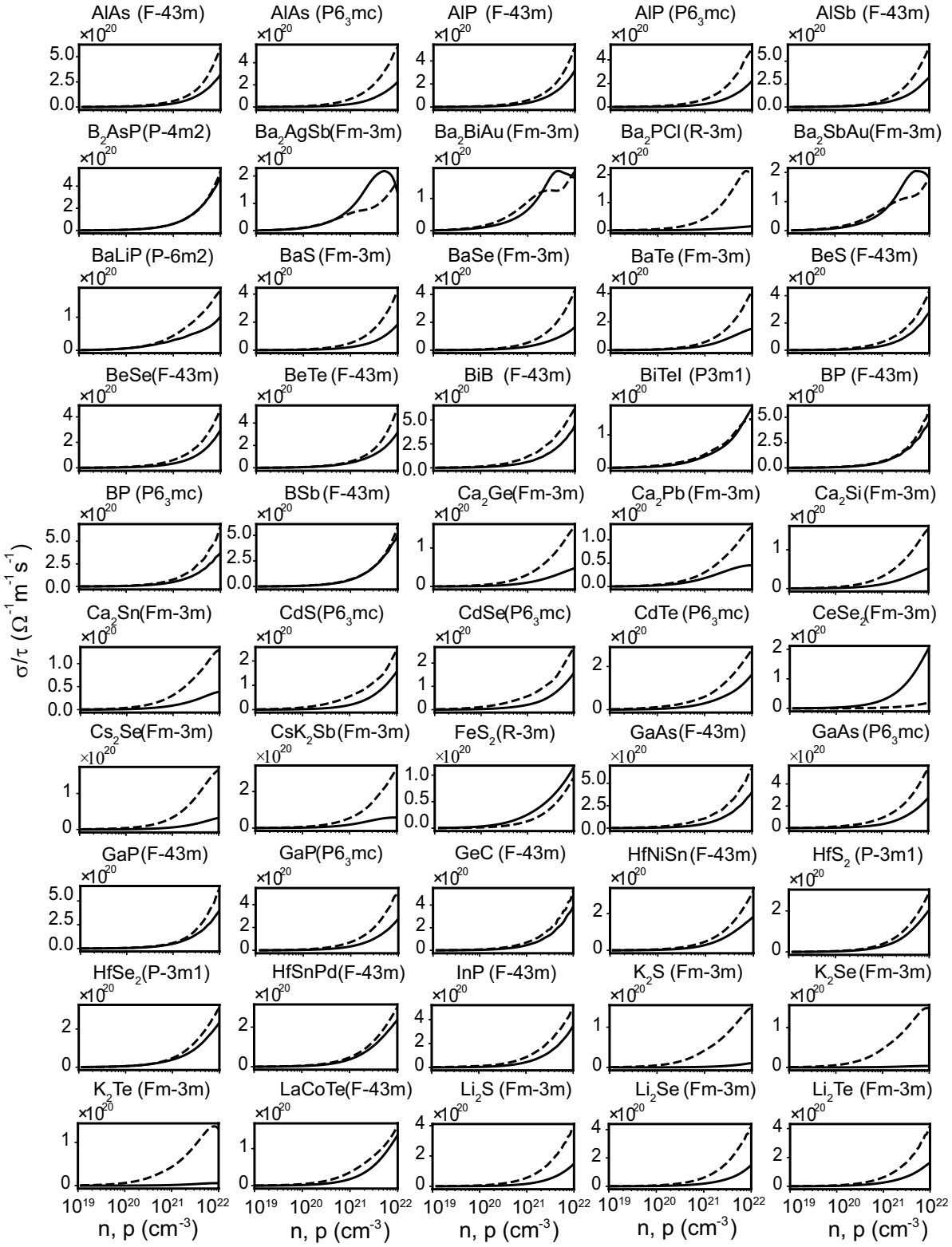

Figure 4: Calculated scaled electrical conductivity σ/τ as a function of carrier concentration at room temperature.

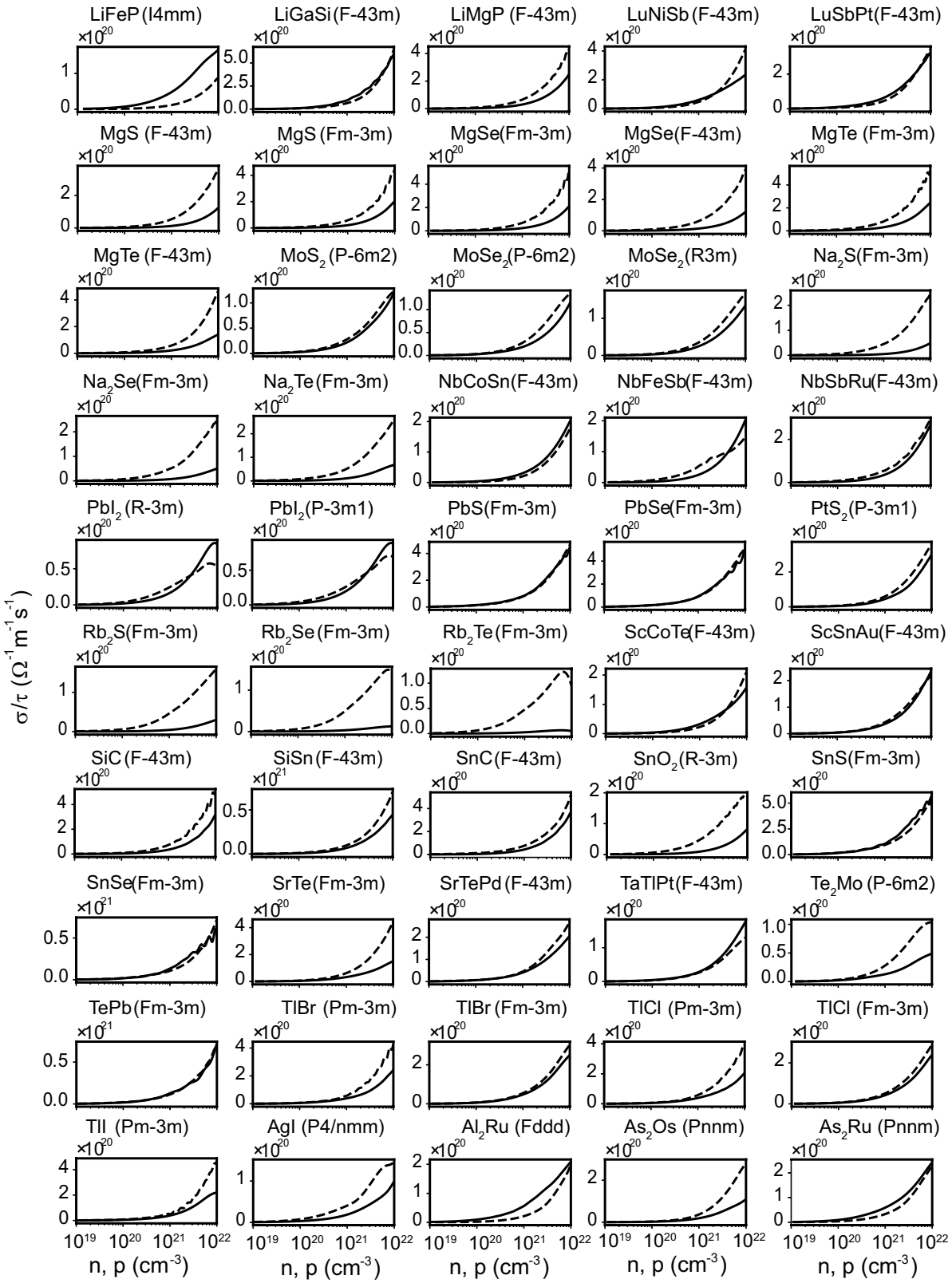

Figure 5: Calculated scaled electrical conductivity σ/τ as a function of carrier concentration at room temperature.

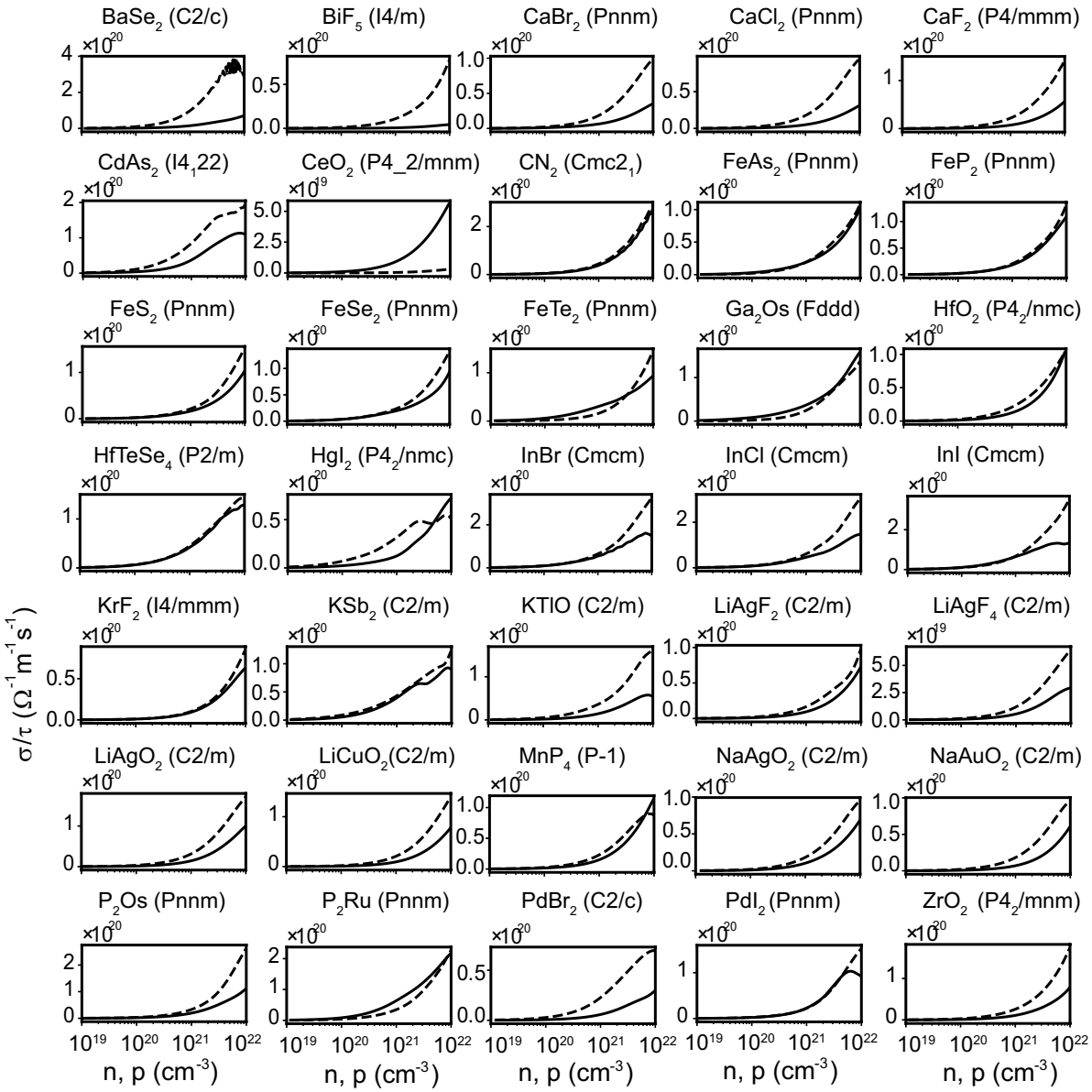

Figure 6: Calculated scaled electrical conductivity σ/τ as a function of carrier concentration at room temperature.

Compounds with ultrahigh powerfactor

By employing the high-throughput screening on the dataset, we found a total of 34 compounds with simultaneously high Seebeck coefficient and electrical conductivity, resulting in very high powerfactor. The scaled powerfactor for these 34 compounds is shown in Figure S7.

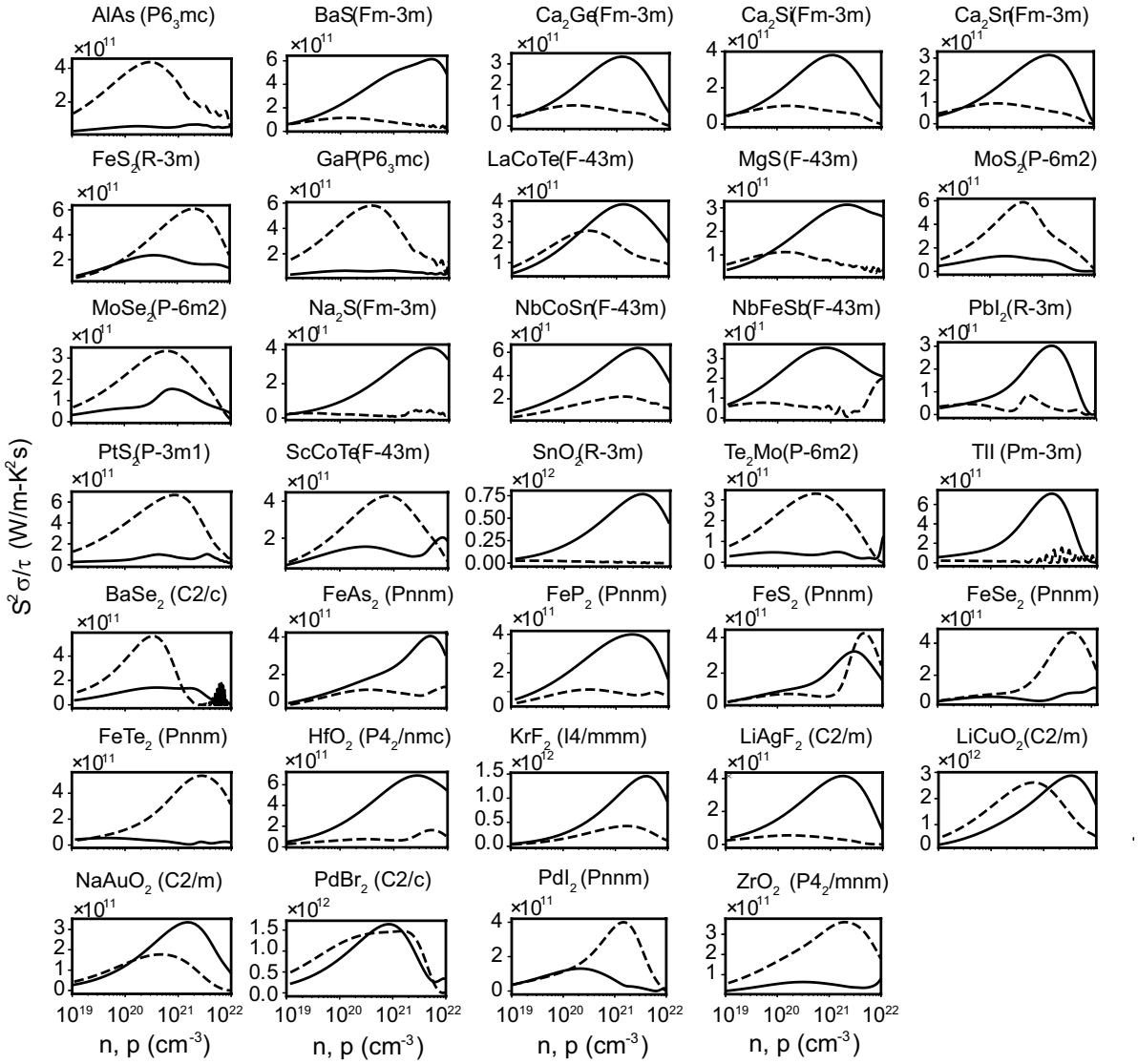

Figure 7: Scaled powerfactor as a function of carrier concentration at room temperature for the 34 compounds with simultaneously high Seebeck coefficient and scaled electrical conductivity resulting in high scaled powerfactor.

Lattice thermal conductivity of compounds with ultrahigh powerfactor

The compounds with ultrahigh powerfactor can be explored for thermoelectric applications if they also possess low lattice thermal conductivity. The room temperature lattice thermal conductivity for the 34 compounds is shown in Table S1.

Table 1: Lattice thermal conductivity of 34 compounds having high powerfactor at T = 300 K

Compound	κ_l (W/mK) at T = 300 K
AlAs ($P6_3mc$)	54.05
BaS (Fm-3m)	6.13
Ca_2Ge (Fm-3m)	5.11
Ca_2Si (Fm-3m)	7.01
Ca_2Sn (Fm-3m)	5.11
$CeSe_2$ (Fm-3m)	5.55
FeS_2 (R-3m)	36.94
GaP ($P6_3mc$)	121.25
LaCoTe (F-43m)	0.978
MgS (F-43m)	26.21
MoS_2 (P-6m2)	108.57
$MoSe_2$ (P-6m2)	21.66
Na_2S (Fm-3m)	5.76
NbCoSn (F-43m)	18.67
NbFeSb (F-43m)	26.35
PbI_2 (R-3m)	0.51
PtS_2 (P-3m1)	99.66
ScCoTe (F-43m)	14.79
SnO_2 (R-3m)	22.43
Te_2Mo (P-6m2)	14.57
TlI (Pm-3m)	0.15
$BaSe_2$ (C2/c)	0.83
$FeAs_2$ (Pnnm)	38.35
FeP_2 (Pnnm)	82.21
FeS_2 (Pnnm)	80.29
$FeSe_2$ (Pnnm)	34.40
$FeTe_2$ (Pnnm)	18.06
HfO_2 ($P4_2/mnm$)	4.72
KrF_2 (I4/mmm)	3.65
$LiAgF_2$ (C2/m)	6.17
$LiCuO_2$ (C2/m)	18.82
$NaAuO_2$ (C2/m)	15.79
$PdBr_2$ (C2/c)	1.85
PdI_2 (Pnnm)	0.44
ZrO_2 ($P4_2/mnm$)	12.52

Independent machine learning models for Seebeck coefficient and scaled electrical conductivity

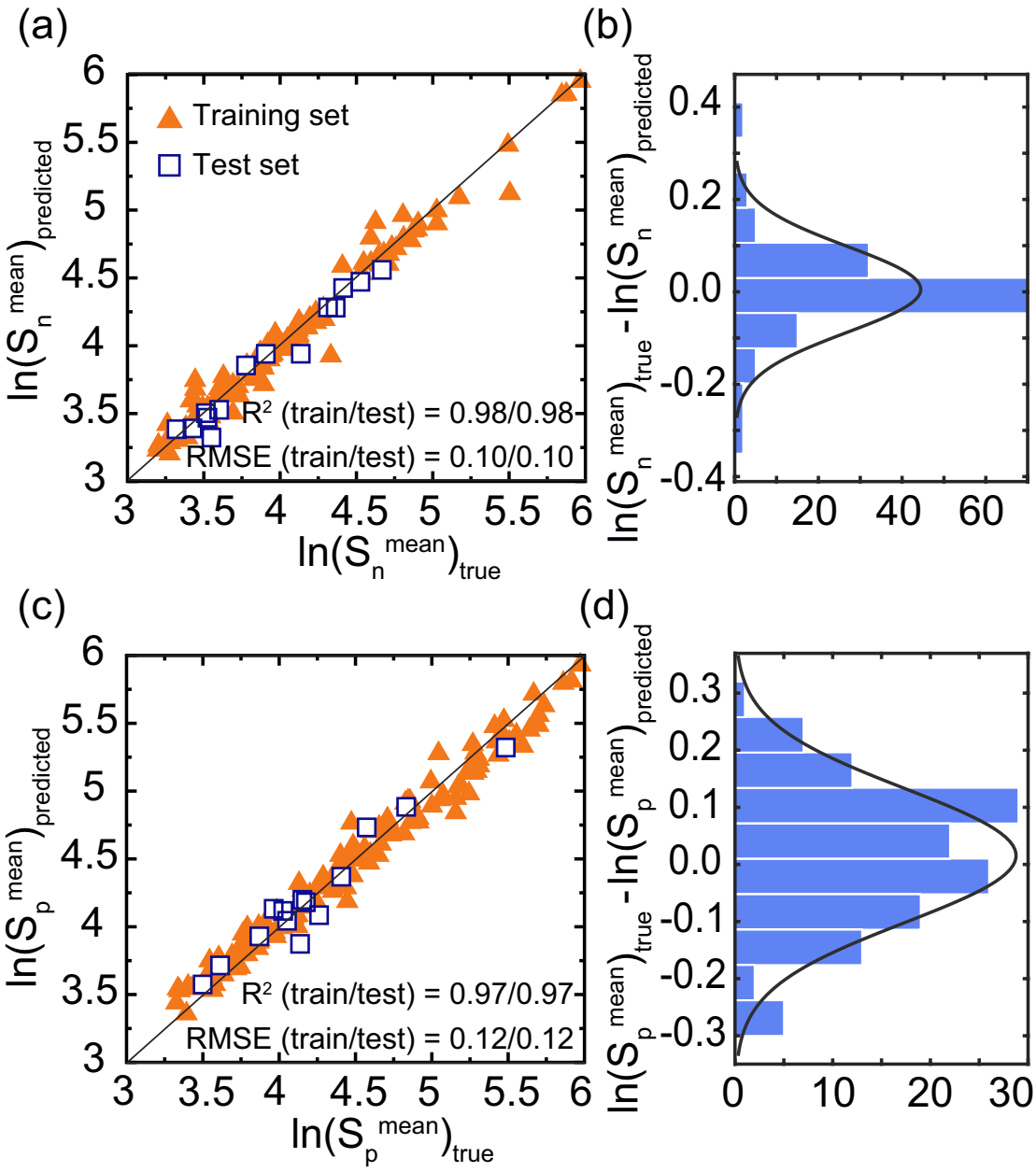

Figure 8: The scatter plot of true versus predicted log-scaled mean of S at room temperature over the carrier concentration range 10^{19} to 10^{22} cm^{-3} for the training and test set for (a) *n*-type carriers and (c) *p*-type carriers. (b) and (d) represent corresponding residual plots.

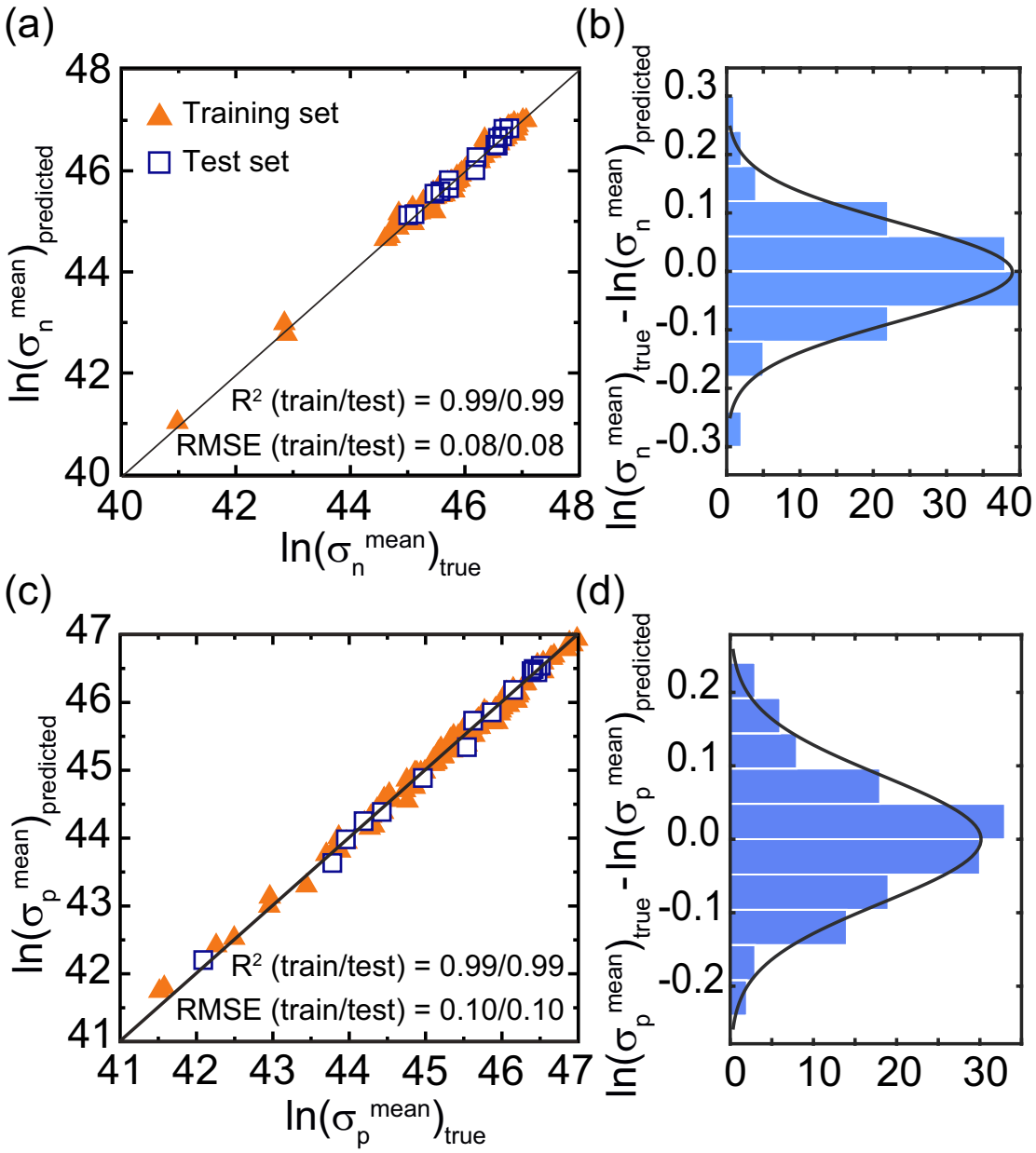

Figure 9: The scatter plot of true versus predicted log-scaled mean of $\frac{\sigma}{\tau}$ at room temperature over the carrier concentration range 10^{19} to 10^{22} cm^{-3} for the training and test set for (a) *n*-type carriers and (c) *p*-type carriers. (b) and (d) represent corresponding residual plots.

Correlation of compound descriptors with lattice thermal conductivity

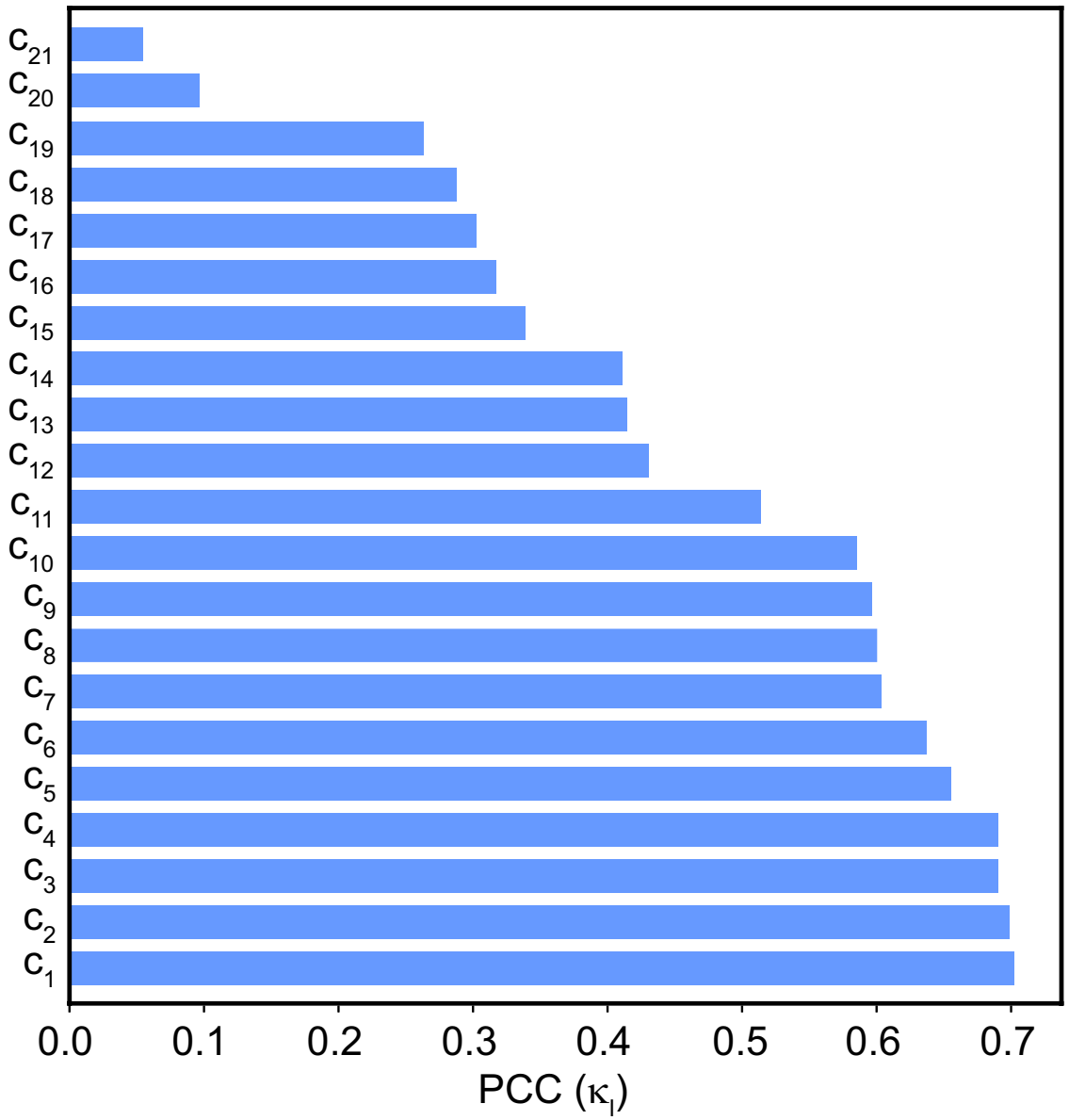

Figure 10: Pearson correlation of compound descriptors with lattice thermal conductivity.

Table 2: Description of compound descriptors

Compound descriptor label	Formula
c_1	$exp(B.D. + V_{cell} + \chi_p^{mean})$
c_2	$exp(\frac{\sigma}{\tau}{}_n^{mean} + B.S.)\frac{1}{exp(B.D.)}$
c_3	$exp(\frac{\sigma}{\tau}{}_n^{mean} + S_n^{std})\frac{1}{exp(B.D.)}$
c_4	$exp(B.D.) + \chi_p^{std}\frac{1}{exp(S_p^{mean})}$
c_5	$exp(B.D.) + \chi_p^{std}\frac{1}{exp(S_p^{std})}$
c_6	$exp(\frac{\sigma}{\tau}{}_n^{mean} + B.S.)\frac{1}{exp(\chi_p^{std})}$
c_7	$B.D.exp(\frac{\sigma}{\tau}{}_n^{mean})exp(\chi_p^{mean})$
c_8	$exp(B.D.)exp(\chi_p^{mean} + \chi_p^{std})$
c_9	$exp(\frac{\sigma}{\tau}{}_n^{mean} + S_n^{std})\frac{1}{V_{cell}}$
c_{10}	$exp(\frac{\sigma}{\tau}{}_n^{mean} + \frac{\sigma}{\tau}{}_n^{std})\frac{1}{exp(B.D.)}$
c_{11}	$B.D.^3exp(B.D. + V_{cell})$
c_{12}	$exp(\frac{\sigma}{\tau}{}_n^{mean} + B.S. + C.N.)$
c_{13}	$exp(\frac{\sigma}{\tau}{}_n^{mean} + S_n^{std} + \frac{\sigma}{\tau}{}_n^{std})$
c_{14}	$exp(\frac{\sigma}{\tau}{}_n^{mean} + B.D. + V_{cell}$
c_{15}	$exp(S_p^{std} + C.N. + \chi_p^{std})$
c_{16}	$exp(\frac{\sigma}{\tau}{}_p^{mean} + B.D. + C.N.)$
c_{17}	$B.S.^3exp(S_n^{std} + B.S.)$
c_{18}	$C.N.^3exp(\frac{\sigma}{\tau}{}_p^{mean} + C.N.)$
c_{19}	$exp(\frac{\sigma}{\tau}{}_p^{mean} + B.D. + \chi_p^{mean})$
c_{20}	$exp(S_p^{mean} + S_n^{std} + S_p^{std})$
c_{21}	$(\chi_p^{mean})^3exp(exp(S_p^{std} + \chi_p^{mean})$